

An Implementation of Battery Charging Methods for Electric Transportation Application

¹K. Thenmozhi,

²Mrs. P. Chandra and ³K. Anbarasan

¹P.G Scholar, Department of Power Electronics and Drives,

^{2,3}Assistant Professor, Department in Electrical and Electronics Engineering,

^{1,2,3}Professor, Dhanalakshmi Srinivasan Engineering College, Perambalur, Tamilnadu, India

Abstract: A dual-inverter with an open-end winding motor arrangement is an attractive system to supply a higher voltage to a motor for electric motor vehicle (EV) applications. A topology utilizing two isolated dc sources. Although this design may need two battery chargers, in this study, the use of only one charger to a main battery was considered. The fundamental problem is to charge the secondary battery from the main battery by way of the motor, whether it is at a standstill or running. The results show that the proposed method is able to noticeably improve the power capability of the motor beyond its base speed. The unity-power-factor operation is shown to be useful to maximize the charging power. The proposed method is extensively simulated in simulated in MATLAB/SIMULINK.

Key words: Battery charging • Dual-inverter • Electric vehicle (EV) • Inner permanent-magnet synchronous motor (IPMSM) • Open-end winding device • Unity-power-Factor (UPF) • Impedance source inverter (ZSI) • Fuzzy logic

INTRODUCTION

Electric vehicles (EV) and connect hybrid electric vehicles (PHEV) are recognized as the future of the automotive industry. In the coming decade the transition to EVs and PHEVs will reduce our national dependence on foreign sources of oil, improve the health of our citizens and environment and create a new clean energy economy. Furthermore these new vehicles will offer better performance with lower fuel and maintenance costs.

The Z-source inverter [1] provides another means to increase the inverter output voltage without using a separate boosting stage. The Z-source inverter, however, requires two bulky capacitors and inductors and the boosting ratios are limited by the output voltage and shoot-through zero state. A dual-inverter with an open-end winding motor arrangement is one method to supply a higher voltage to the machine [2-8]. Typically, two inverters are connected to both terminals of an open-end

winding motor. Though it requires six additional switches, the increased voltage output leads to high efficiency in a high-speed region.

In [9-14], a motor control scheme for a dual-inverter with a floating capacitor bridge has been developed. However, this scheme provides only a reactive voltage component from the secondary inverter to the motor. [15], [16] proposed a series hybrid power trains based on an open-winding machine drive. An open-end winding permanent magnet (PM) generator was coupled to an internal combustion engine (ICE) and the generated control was dividing into two isolated dc buses through individual rectifiers. Two popular topologies for the dual-inverter drive system are shown in Fig. 1 with the related voltage vector hexagons. In Fig. 1(a), two dc links are connected to a single voltage source. However, two separate voltage sources are utilized in Fig. 1(b). Note in the case of a single voltage source that a substantial amount of a triplen harmonic current is caused by a triplen harmonic voltage. For this reason, many research efforts

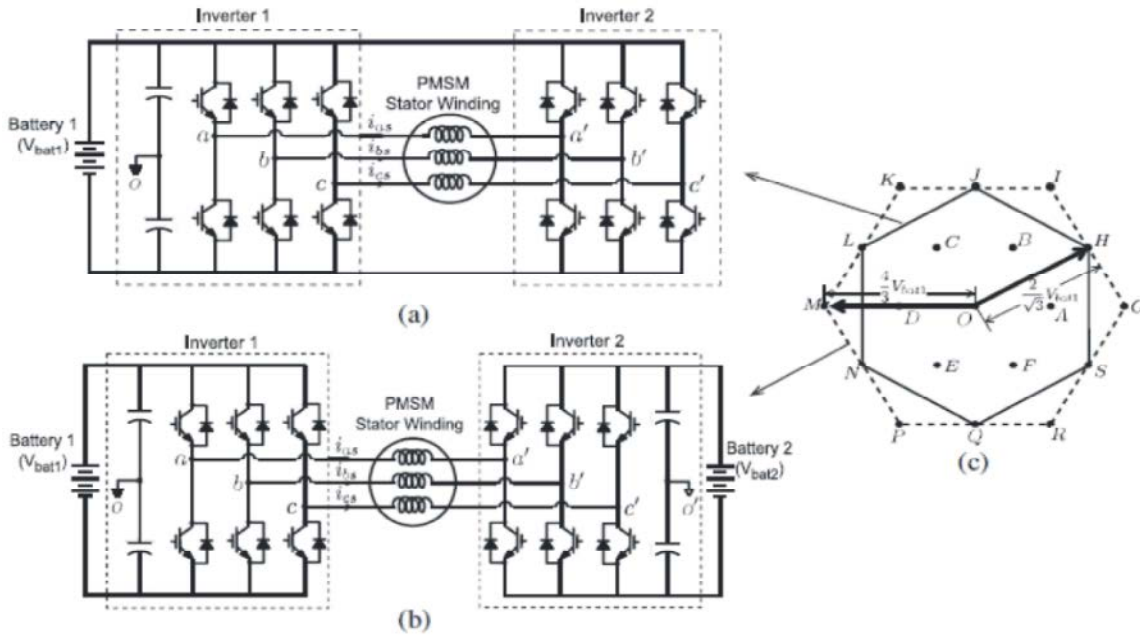


Fig. 1: Configuration of dual-inverter system (a) single voltage source, (b) isolated dual voltage source and (c) Related voltage vector hexagon

in the field of open-winding motor drives have been used up on pulse width modulation (PWM) techniques to suppress the triplen harmonic current [17-24].

Two insulated dc supplies inherently eliminate the common mode voltage and current [25, 26], thereby no limitation is imposed on PWM switching. Furthermore, this topology offers a highly reliable solution. In fact, in case of a fault in one inverter, its output terminals can be short-circuited and the system can work using a healthy inverter as a standard three phase two-level inverter [27].

In fact, in case of a fault in one inverter, its amount produced terminals can be short-circuited and the system can operate using a healthy inverter as a standard three phase two-level inverter [28]. The EV application of a dual supply Inverter and consider using one charger for the dual source inverters. In this existing scheme, only Battery 1 is charged by an peripheral charger. Battery 2 is charged via Inverters 1 and 2 from Battery 1. in this system produced the main limitation to accelerating adoption of these new vehicles has been their initial cost high. Primarily due to the cost of lithium ion battery systems. [29]

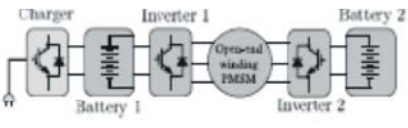
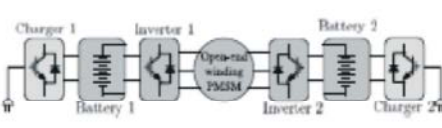
Dual Inverter Fed Induction Motor Through Open-end Winding: A representation of an open-end winding induction coast is shown in Fig. 1 both inverter can

produce its own voltage space Phasor locations, resulting in a joint voltage space Phasor locations and combinations as shown in Fig. 2. There are a whole of 64 breathing space Phasor combinations possible from the constrain scheme of Fig. 1. But due to the open-end winding structure for the motor, the drive system of Fig. 1 is able to introduce substantial number roof triple harmonic currents in the motor phase windings. A comprehensive analysis of triplen harmonic contributions from various space Phasor combinations is presented. In a three-level PWM control for the open-end winding drive is achieve by introduce a switched neutral with supplementary bidirectional switches (Fig. 3). This will result in reduced DC link utilization, because the intense vertices of Fig. 2 are not used for PWM operation. In the present work, full DC link utilization is achieved by properly controlling the auxiliary winding bidirectional switches. The resulting in operation similar to conventional three-level PWM operation.

For the 3-5' combination the motor phase voltages are:

$$\begin{aligned}
 V_{aa}' &= V_{a'o} - V_{a'o} = -V_{dc}/4 - (-V_{dc}/4) = 0 \\
 V_{bb}' &= V_{b'o} - V_{b'o} = +V_{dc}/4 - (-V_{dc}/4) = V_{dc}/2 \\
 V_{cc}' &= V_{c'o} - V_{c'o} = -V_{dc}/4 - (-V_{dc}/4) = -V_{dc}/2
 \end{aligned}
 \tag{1}$$

Table 1: Advantage/disadvantage of One Charger Method Against Two Charger Method

	One charger method	Two charger method
Configuration		
Cost	Low	High
Weight	Low	High
Charging efficiency	low	High
User convenience	Good	Poor

The triplen harmonic voltage is given by:

$$V_{triplen} = (V_{aa'} + V_{bb'} + V_{cc'})/3 \quad (2)$$

For the combination 3-5' the triplen harmonics content is calculated as,

$$V_{triplen} (3-5)' = (V_{aa'} + V_{bb'} + V_{cc'})/3 \quad (3)$$

Battery Charging Methods for Dualinverter System:

Battery 2 is an auxiliary battery that can be used as an assistant voltage source when a high voltage is necessary for a motor operation. In the low-speed range, Battery 1 acts as the main power source and Battery 2 is shut down by setting a 0 or 7 vector at Inverter 2. At a high speed, Inverter 2 contributes to increasing the supply voltage to the motor in series with Inverter 1. Hence, the use of Battery 2 is not continuous but intermittent. Whenever the voltage level is low, it needs to be charged for later operation. First, we consider a method of charging Battery 2 when the motor is under 1) the stationary state, 2) low speed operation and 3) high speed operation. charged for later operation. First, we consider a method of charging Battery 2 when the motor is under 1) the stationary state, 2) low speed operation and 3) high speed operation.

Operating Principle: Operation of the double-ended inverter system can be broken down into two parts as covered in the following sections. The first part consists of the mathematical system model. From the system model, the resultant power flow in the system can be determined.

System Modeling: The double-ended inverter consists of two three-phase inverters that are fed by electrically

isolated dc sources. They will be referred to as inverter one (INVR1) and inverter two (INVR2). The inverters are connected to an open end-winding motor. The two sources may have different voltage amplitudes. From Fig. 1, the motor phase voltages can be;

$$v_a = v_{a1g1} + v_{g1g2} - v_{a2g2} \quad (4)$$

$$v_b = v_{b1g1} + v_{g1g2} - v_{b2g2} \quad (5)$$

$$v_c = v_{c1g1} + v_{g1g2} - v_{c2g2}. \quad (6)$$

Since the two inverters are electrically isolated from one another, the two grounds can be thought of as independent nodes in the circuit. As a result, the motor phase currents employing Kirchhoff's law are given as;

$$i_a + i_b + i_c = 0 \quad (7)$$

This further implies a similar relationship for the motor phase;

Voltages, given as ,

$$v_a + v_b + v_c = 0. \quad (8)$$

Control Methods: For purposes of determining the required voltage and current calculations to control the power flow, it is useful to simplify the system of Fig. 1 to that of a one-line diagram or per-phase equivalent circuit, as shown in Fig. 4. Essentially, the double-ended inverter can be thought of as two ac sources connected through a common load. From Kirchhoff's voltage law.

$$V^{\circ}dq = V^{\circ}dq1 - V^{\circ}dq2 \quad (9)$$

Unity Power Factor Control: One technique to control the power output of the battery powered INVR2 is to operate that inverter with union power factor while controlling its output voltage amplitude. This will maximize the energy flow in INVR2. The phasor diagram for this method is shown in Fig. 5. In Fig. 5a, the secondary source supplied converter is outputting a voltage 180° out of point with the load current. This represents a situation where the battery is supplying power to the load with a concord power factor. It is significant to recall the minus sign in (11), due to the current and voltage definitions, which consequences in the out of phase condition. The total voltage useful to the load is also shown in the figure. Fig. 5b shows the phasor diagram for the same load current and load voltage state, except that now the secondary source is absorbing control or being charged. As a result, the necessary voltage output of the primary source converter has been increased. In order to regulate the secondary source power, assume that INVR2 is being operated at unity power factor. Therefore,

$$V^{e}_{dq1^*} = V^{e}_{dq} + V^{e}_{dq2^*} \tag{10}$$

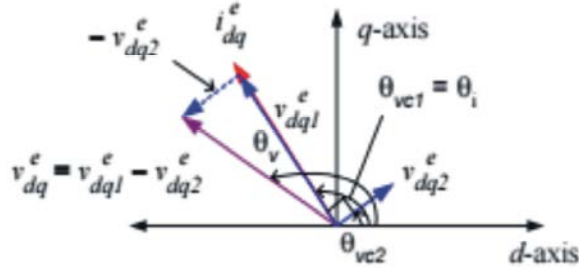


Fig. 2: INVR2 (battery) operating in quadrature

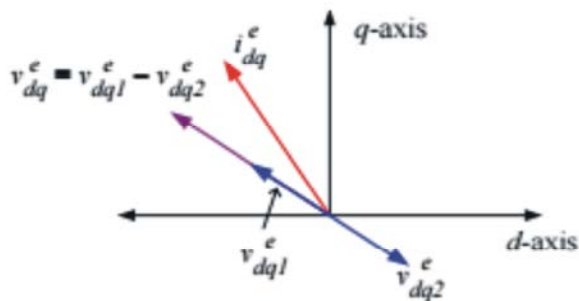


Fig. 3: Phasor diagram with INVR1 and INVR2 Producing maximum output

Optimum Inverter Utilization Control: The greatest harvest voltage of the double-ended inverter system (as seen by the load) occurs when the two converters are each outputting their most phase voltage, with the phase voltages out of phase by 180° . The phasor figure for this control technique is shown in Fig. 4.

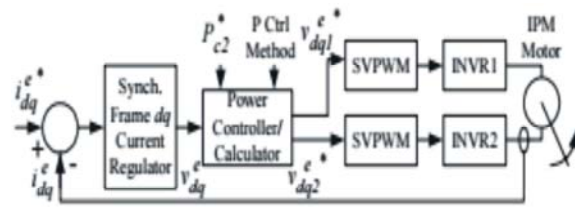


Fig. 4: Control block diagram

For the optimum inverter utilization control, the output voltages of the inverters are co-linear. As a result, essential voltages are simply proportional to the desired power. Therefore, the battery powered INVR2 commands are

To increase the utilization of fuel cells and to avoid dreading of semiconductors, this paper proposes a level reduction control using a multilevel inverter. Level decrease is done by inhibiting a certain number of fuel cells when the load current decreases. The withdrawn fuel cells can be used in other applications such as charging batteries to additional increase their utilization and the efficiency of the scheme.

Proposed Modulation: The system consists of Input battery, output storage battery, ZSI, PMSM open end winding, CSI based converter, with MOSFET driver and Micro-controller. ZSI is used to extend the voltage from battery. And it used to perform DC-AC conversion. It consists of 2 identical inductors and 2 identical capacitor. The Current source inverter is a boost inverter for dc-to-ac power exchange with the I-source converter is a buck rectifier (or buck converter) for ac-to-dc power conversion. MOSFET driver used to amplify the indicator from Micro-controller. Reactive power is optimized by using Fuzzy logic. At the same time THD also reduced. Fuzzy logic controller is used for proposed system.

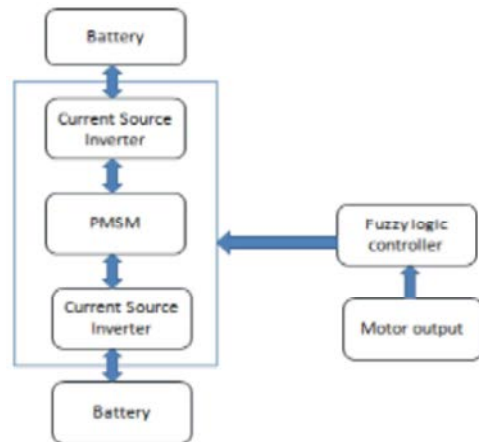


Fig. 5: Block Diagram

Block Diagram Description: The input voltage, output electrical energy and regularity and overall power handling depend on the plan of the specific device or circuitry. The inverter does not construct any power; the power is provided by the DC source. Three-phase inverters are used for unpredictable-frequency drive applications and for high control applications such as HVDC power transmission. A critical three-phase inverter consists of three single phase inverter switches each linked to one of the three load terminals. For the majority fundamental control scheme, the operation of the three switches is corresponding so that one switch operates at each 60 degree peak of the essential output waveform.

Working of Fuzzy Logic Controller: Fuzzy control has emerged as a sensible alternative to conventional control schemes when one is concerned in controlling confident time changeable, non-linear and ill-defined processes. There have in fact been more than a few successful commercial and industrial applications of fuzzy control. Fuzzy controllers are used to control purchaser yield, such as washing machinery, record cameras and rice cookers, as well as industrial processes, such as cement kilns, subversive trains and robots. Fuzzy control is a control method based on fuzzy logic. Fuzzy logic can be describe purely as computing with words quite than numbers; fuzzy control can be described basically as control with sentences slightly than equations. A fuzzy controller can contain empirical system and that is particularly valuable in operative forbidden plant life.

Open-Winding PMSG System: A 1.7-kW open-winding PMSG was experienced in this part of the research Parameters of the open-winding PMSG can be established in the appendix. The back EMF mostly consists of 3.03 V/Hz fundamental, 12.3% third harmonic and 0.6% fifth harmonic.

Dual Inverter: The open stator windings are connected to the legs of *Inv1* and *Inv2*. *Inv1* connected to the battery is drawn at the left side of Fig. 6 and *Inv2* connected to the capacitor bank is at the opposite end. Terminals and switches of the *Inv2* are expressed with prime for easy contrast.

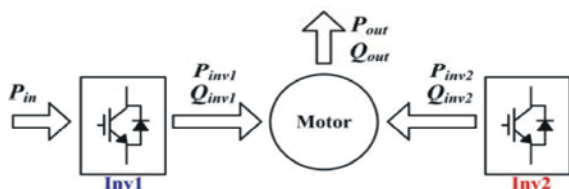


Fig. 6: Power flow diagram of dual inverter system

Fig. 6 shows power flow diagram of dual inverter driven machine. Active powers are indicated with *P* and reactive powers are indicated with *Q*. Because motor is fed by two inverters, power flow equations can be written as,

$$\begin{aligned} P_{out} &= P_{inv1} + P_{inv2} \\ Q_{out} &= Q_{inv1} + Q_{inv2} \end{aligned} \quad (11)$$

Table 2: Summary of Dual Inverter Topologies

Topology	Figure	Maximum phase voltage	Notes
Single inverter with boost converter	Fig. 1(a)	$V_{dc}/\sqrt{3}$	Inductor is required
Dual inverter with common DC link	Fig. 1(b)	V_{dc}	0 common mode voltage
Dual inverter with isolated DC links	Fig. 1(c)	$(V_{dc1} + V_{dc2})/\sqrt{3}$	Differential mode power transfer
Dual inverter with common mode connected DC links	Fig. 1(d)	$(V_{dc1} + V_{dc2})/2$	Common mode power transfer

So, its linearly available phase voltage is $(V_{dc1} + V_{dc2})/2$ when Common mode current is controlled to 0. Thanks to the common mode path, it is tougher to the EMI and wear of bearing which comes from common mode parasitic components. Because only one inverter is connected to the power source, another inverter has to be left in flying.

It is obvious that the voltage of the flying DC link is defined by active power flow through the flying inverter. Because DC link voltage should be controlled stable, active power flow to the flying DC link should be controlled to 0. Although it is Impossible to supply continuous active power, however, Reactive power can be supplied to the motor from the flying Inverter. Reactive power source.

Polevoltages of *Inv1* are V_{ao} , V_{bo} , and V_{co} , and polevoltages of *Inv2* are $V_{a'o}$, $V_{b'o}$, and $V_{c'o}$. Phasevoltages applied to the motor are expressed as;

$$\begin{aligned} V_{aa} &= V_{ao} - V_{a'o} + V_{c'o} \\ V_{bb} &= V_{bo} - V_{b'o} + V_{c'o} \\ V_{cc} &= V_{co} - V_{c'o} + V_{a'o} \end{aligned} \quad (12)$$

Simulation Results: The Gate signals generated by the DSP and experimentally obtained waveforms of the A-phase pole voltages of the two inverters, the A-phase motor-phase voltage, the zero-sequence voltage, the normalized harmonic spectra of the difference in pole voltages and the no-load motor-phase current for a modulation index (*mi*).

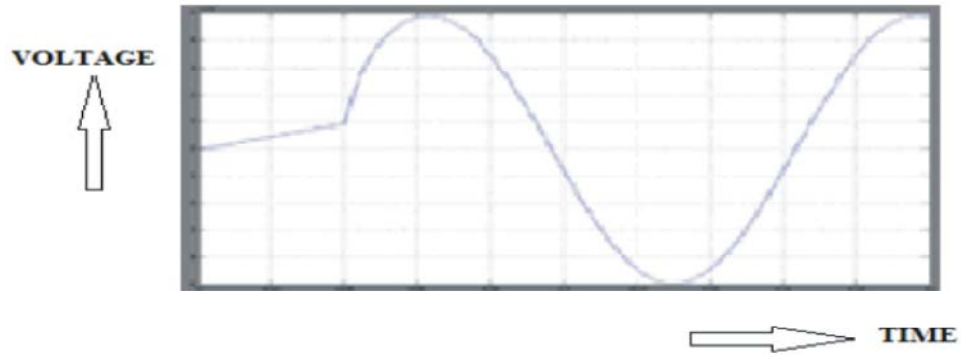


Fig. 8: Simulation Diagram for PWM Inverter Voltage

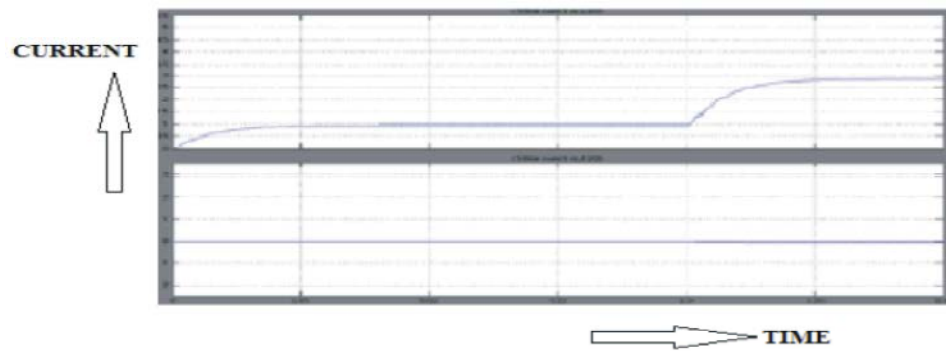


Fig. 9: Simulation Diagram for Stator Current

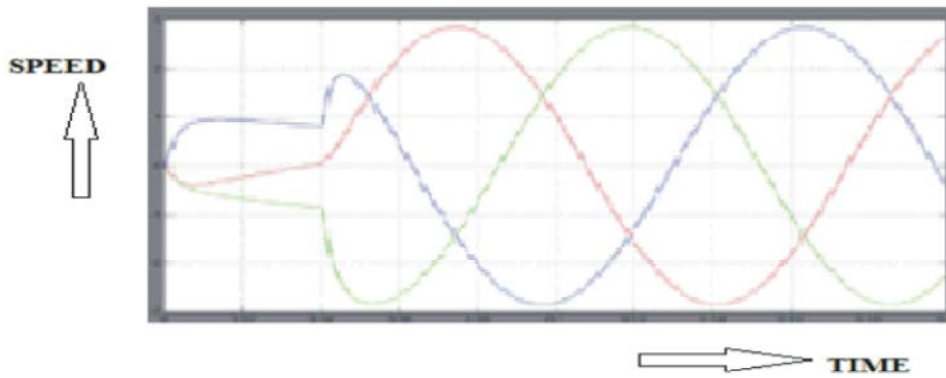


Fig. 10: Simulation Diagram for Rotor Speed

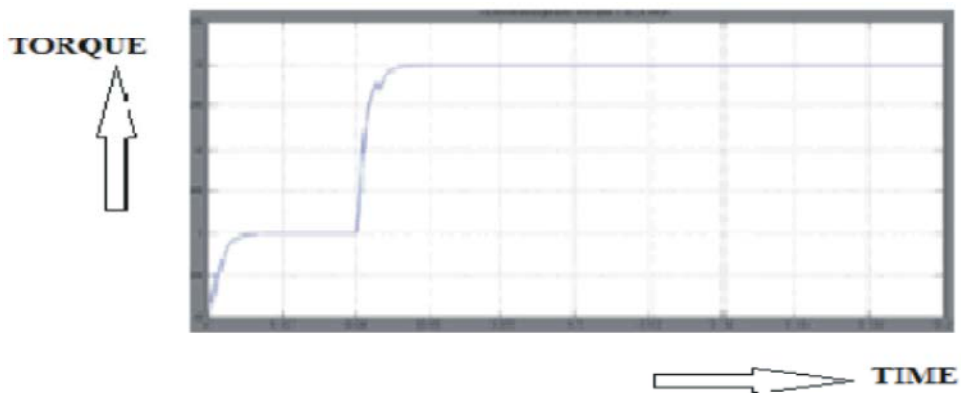


Fig. 11: Simulation Diagram for Electro Magnetic Torque

CONCLUSION

A battery charging method was proposed for a dual-inverter drive system with an open-end winding IPMSM. Throughout the paper, a secondary battery charging method was considered. The charging scheme covered the whole speed range of the motor at a standstill, in the low-speed region and in the field weakening region. At a standstill, only the d-axis current was used for charging in order to not produce a torque. In the field weakening region, the operating point was moved along the constant-torque line to a tangential intersection with a voltage limit curve to gain a potential to charge the battery. Furthermore, it was shown that the unity power factor operation of Inverter 1 yielded the maximum power to Battery 2. Evidence from the simulation and experiments was provided that demonstrated the effectiveness of the proposed charging scheme.

REFERENCES

1. Peng, F.Z., 2003. "Z-source inverter," IEEE Trans. Ind. Appl., 39(2): 504-510.
2. Stemmler, H. and P. Guggenbach, 1993. "Configurations of high-power voltage source inverter drives," in Proc. Fifth Eur. Conf. Power Electron. Appl., 5: 7-14.
3. Stemmler, H., 1994. "High-power industrial drives," Proc. IEEE, 82(8): 1266-1286.
4. Kawabata, T., E.C. Ejiogu, Y. Kawabata and K. Nishiyama, 1997. "New openwinding configurations for high power inverters," in Proc. IEEE Int. Symp. Ind. Electron., 2: 457-462.
5. Kawabata, Y., M. Nasu, T. Nomoto, E.C. Ejiogu and T. Kawabata, 2002. "High efficiency and low acoustic noise drive system using open-winding AC motor and two space-vector-modulated inverters," IEEE Trans. Ind. Electron., 49(4): 783-789.
6. Corzine, K.A., S.D. Sudhoff and C.A. Whitcomb, 1999. "Performance characteristics of a cascaded two-level converter," IEEE Trans. Energy Convers., 14(3): 433-439.
7. Welchko, B.A. and J.M. Nagashima, 2003. "The influence of topology selection on the design of EV/HEV propulsion systems," IEEE Power Electron. Lett., 1(2): 36-40.
8. Kwak, M.S. and S.K. Sul, 2007. "Flux weakening control of an open winding machine with isolated dual inverters," in Proc. Ind. Appl. Conf., pp: 251-55.
9. Kim, J., J. Jung and K. Nam, 2004. "Dual-inverter control strategy for high-speed operation of EV induction motors," IEEE Trans. Ind. Electron., 51(2): 312-320.
10. Ewanchuk, J., J. Salmon and C. Chapelsky, 2013. "A method for supply voltage boosting in an open-ended induction machine using a dual inverter system with a floating capacitor bridge," IEEE Trans. Power Electron., 28(3): 1348-1356.
11. Park, J.S. and K. Nam, 2006. "Dual inverter strategy for high speed operation of HEV permanent magnet synchronous motor," in Proc. IEEE Ind. Appl. Conf., 1: 488-494.
12. Pan, D., F. Liang, Y. Wang and T.A. Lipo, 2012. "Extention of the operating region of an IPM motor utilizing series compensation," in Proc. IEEE Energy Convers. Congr. Expo., pp: 823-830.
13. Lee, Y. and J.I. Ha, 2013., "Power enhancement of dual inverter for open-end permanent magnet synchronous motor," in Proc. IEEE Appl. Power Electron. Conf. Expo., pp: 1545-1551.
14. Lee, Y. and J.I. Ha, 2013. "Six step phase modulation of dual inverter for open end permanent magnet synchronous motor," in Proc. Energy Convers. Congr. Expo., pp: 3874-3879.
15. Welchko, B.A., 2005. "A double-ended inverter system for the combined propulsion and energy management functions in hybrid vehicles with energy storage," in Proc. IEEE 31st Annu. Conf. Ind. Electron. Soc., Raleigh, NC, USA, Nov. 6-10, pp: 1401-1406.
16. Rossi, C., G. Grandi and P. Corbelli, 2008. "Series hybrid powertrain based on the dual two-level inverter," in Proc. Optim. Electr. Electron. Equipment OPTIM, Brasov, Romania, pp: 277-286.
17. Rossi, C., G. Grandi, P. Corbelli and D. Casadei, 2009. "Generation system for series hybrid powertrain based on dual two-level inverter," in Proc. Eur. Power Electron. Appl. Conf., Barcelona, Spain, 2009.
18. Somasekhar, V.T., K. Gopakumar, A. Pittet and V.T. Ranganathan, 2002. "PWM inverter switching strategy for a dual two-level inverter FED open-end winding induction motor drive with a switched neutral," IEE Proc., Electr. Power Appl., 149: 152-160.
19. Somasekhar, V.T., M.R. Baiju and K. Gopakumar, 2004. "Dual two level inverter scheme for an open-endwinding induction motor drivewith a single dc power supply and improved dc bus utilization," Proc. Inst. Electr. Eng. Electr. Power Appl., 151(2): 230-238.

20. Shivakumar, E.G., K. Gopakumar, S.K. Sinha, A. Pittet and V.T. Ranganathan, 2000. "Space vector PWM control of dual inverter FED open-end winding induction motor drive," Proc. IEEE 16th Ann. Appl. Power Electron. Conf. Expo., pp: 394-404.
21. Oleschuk, V., F. Profumo, G. Griva, R. Bojoi and A.M. Stankovic, 2006. "Analysis and comparison of basic schemes of synchronized PWM for dual inverter-FED drives," in Proc. IEEE Int. Symp. Ind. Electr., pp: 2455-2461.
22. Kalaiselvi, J. and S. Srinivas, 2013. "Hybrid PWMs for shaft voltage reduction in a dual inverter FED induction motor drive," in Proc. Conf. IEEE Ind. Technol., pp: 539-544.
23. Grandi, G. and D. Ostoic, 2009. "Dual inverter space vector modulation with power balancing capability," in Proc. IEEE Reg. Conf. EUROCON, St. Petersburg, Russia, May 18-23, 2009, pp: 721-728.
24. Baiju, M.R., K.K. Mohapatra, R.S. Kanchan and K. Gopakumar, 2004. "A dual two-level inverter scheme with common mode voltage elimination for an induction motor drive," IEEE Trans. Power Electron., 19(3): 794-805.
25. Somasekhar, V.T., S. Srinivas and K.K. Kumar, 2008. "Effect of zero-vector placement in a dual-inverter FED open-endwinding induction-motor drive with a decoupled space-vector PWM strategy," IEEE Trans. Ind. Appl., 55(6): 2497-2505.
26. Casadei, D., G. Grandi, A. Lega, C. Rossi and L. Zarri, 2007. "Switching technique for dual-two level inverter supplied by two separate sources," in Proc. IEEE Appl. Power Elec. Conf., Anaheim, CA, USA, 2007, pp: 1522-1528.
27. Casadei, D., G. Grandi, A. Lega and C. Rossi, 2008. "Multilevel operation and input power balancing for a dual two-level inverter with insulated dc sources," IEEE Trans. Ind. Appl., 44(6): 1815-1824.
28. Rossi, C., D. Casadei, G. Grandi and A. Lega, 2008. "Multilevel operation and input power balancing for a dual two-level inverter with insulated dc sources," IEEE Trans. Ind. Appl., 44(6): 1815-1824.
29. Jinseok Hong, Heekwang Lee, Kwanghee Nam, 2015. "Charging Method For The Secondary Battery in Dual-Inverter DriveSystems for Electric Vehicles," IEEE Trans. Power Electron, 30: 909-921.